

## Simulation of low-energy x-ray tubes emitted by carbon nanotube field emitter

MuHyeop Cha<sup>a</sup>, Gyuhaeng Jo<sup>a</sup>, Soobin Lim<sup>a</sup>, Se Hoon Gihm<sup>b</sup>, Hyeon Gu Cho<sup>b</sup>, Hyun Jin Kim<sup>b</sup>, KyoungJae Chung<sup>a\*</sup>

<sup>a</sup>Department of Nuclear Engineering, Seoul National University, 1, Kwanak-ro, Kwanak-gu, Seoul, Republic of Korea

<sup>b</sup>aweXome Ray Inc, Anyang, Gyeonggi-Do 14056, Republic of Korea

\*Corresponding author: jkjlsh1@snu.ac.kr

**\*Keywords :** Low energy X-rays, Energy spectrum measurement, Monte Carlo Simulation, Geant4, MCNP6

### 1. Introduction

A low-energy X-ray tube utilizing carbon nanotubes(CNTs) operates as a diode emitting electrons via field emission, interacting with a metal anode to produce X-rays[1,2]. Characterization of X-ray tubes is crucial in designing such devices because it provides an understanding of dose and sanitizing performance. An important factor in representing an X-ray tube's characteristics is the X-ray energy spectrum and fluence intensity. The metal anode acts as both the X-ray generation source and a shielding material, thus influencing both of these factors.

In this study, Geant4 Monte Carlo Simulations are employed to confirm the process of electron beam conversion into X-rays and predict the energy spectrum with respect to anode width[3]. MCNP6 simulation is conducted to cross-check the results[4].

### 2. Simulation setup

This section describes some of the techniques used to model x-ray tubes. After introducing the x-ray tube, the simulation structure and physical models are discussed.

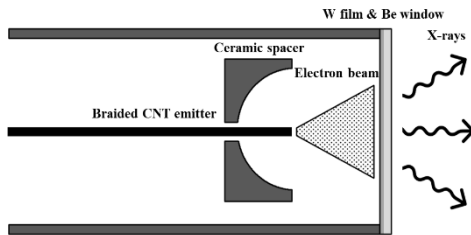


Fig. 1. Example of commercial CNT X-ray Tube. X-ray Tube is a diode using Carbon NanoTubes(CNT) cathode.

#### 2.1 X-ray Source Tube Model

Figure 1 illustrates the simplified structure of the X-ray tube. The tube is a diode device consisting of a carbon nanotube braided tip as a cathode and the tungsten target as the anode. The anode is grounded, while -5 kilovolts are applied to the cathode to induce field electron emission. The emitted electron beam is accelerated and passes through the tungsten target, emitting X-rays as bremsstrahlung or characteristic lines. The emitted X-rays propagate outward, passing through a beryllium window that seals the tube. The

tungsten target is deposited in front of the beryllium window.

A plane electron beam source is assumed instead of implementing a precise field electron emission profile, as depicted in Figure 1. Like Fig. 2, It is assumed that an electron beam with an energy of 5 keV is emitted from the cathode position in a shape the same as the tungsten target.

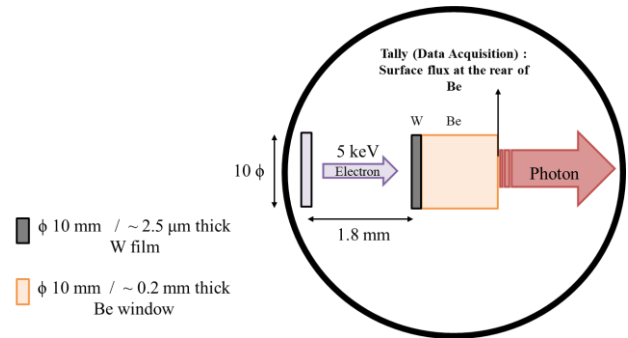


Fig. 2. Schematic view of X-ray Tube modeling. Beam source is assumed a plane electron emitter with 5 keV energy.

#### 2.2 Physics Model

In the Geant4 simulation toolkit, it is necessary to manually input a list of physics reactions that appropriately simulate the situation based on the energy range and the species of the particles used. In this work, we employed Livermore Physics and Penelope Physics[5], both supporting low-energy level physics. These physics models are available for low-energy electromagnetic interactions above 1 keV. Particles with energies below 1 keV is cut-offed. Through these physics models, the typical reactions implemented for converting electrons into X-rays is bremsstrahlung, Electron Ionization, and Coulomb Multiple Scattering in Geant4. In transport simulation, injected electrons behave as macro-particles, secondary particles that cannot travel further than a preset range would not be generated but are simply calculated as energy loss of primary particles. Geant4 provides setcuts for the expected range. Note that too long distance setcuts may result in photons not being generated within tungsten, which also behaves as shielding material. Setcuts is set as 10nm for electrons and photons.

### 2.3 Cross-Checking and Simulation Condition

Cross-checking between the two simulations is conducted for validation of Geant4 physics model. x-ray flux measurements are taken at a position outside the beryllium window of the tube.

The thickness of the tungsten target is varied from 200 nm to 2.5  $\mu\text{m}$  to observe the energy spectrum and the total fluence, where the thickness of the beryllium window is fixed at 200  $\mu\text{m}$ . The scattering angle distribution of X-rays considering only the tungsten target without the beryllium window is obtained. The process of x-ray generation in each energy region is extracted to analyze the spectrum using Geant4.

### 3. Results and Discussion

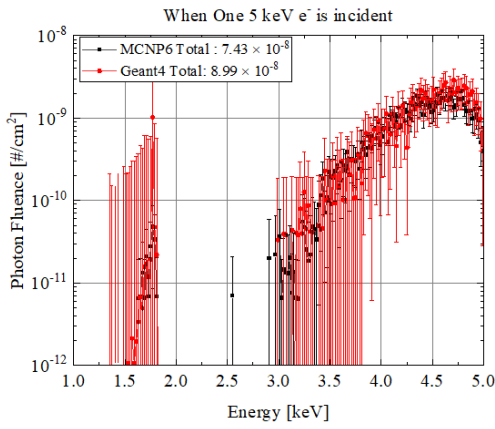


Fig. 3. Energy spectrum of X-ray Tube with 2.5  $\mu\text{m}$  tungsten film and 200  $\mu\text{m}$  beryllium window. The fluences of the two datasets also match well within a 20% error under different anode thickness conditions, from 250 nm to 2.5  $\mu\text{m}$ .

Figure 3 shows the fluence of X-rays measured as a function of energy, taken directly outside the 2.5  $\mu\text{m}$  thick tungsten and 200  $\mu\text{m}$  beryllium window. Statistical error is considered about  $1\sigma$  within the Poisson distribution assumption. The total fluence of MCNP6 and Geant4 is about  $10^{-7} \#/\text{cm}^2$ .

The energy spectrum depicted in Figure 3 shows two distinguishable regions. The hill-shaped region in the right is from bremsstrahlung, the continuous X-ray spectrum. The centroid of the continuum is shifted to the higher energy from its original spectrum due to low energy attenuation by the beryllium target[6]. The left portion of the graph below 2 keV represents the continuous X-ray spectrum. The peak near 2 keV appearing on the left represents the M-line of characteristic x-rays of tungsten ( $M_\alpha = 1.78 \text{ keV}$ ,  $M_\beta = 1.84 \text{ keV}$ ).

Table I shows the probability of generating X-ray photons per unit 5 keV energy electron incident as a function of tungsten target thickness. Both data match well in 20% error. Therefore, it can be concluded that

the physics model applied to the Geant4 toolkit is valid compared to MCNP6.

Table I: Expectation value of x-ray generation per unit incident electron, calculated by MCNP6 and Geant4

Anode width	Fluence ( $\#/\text{cm}^2$ )	
	MCNP6	Geant4
2.50 $\mu\text{m}$	$7.43 \cdot 10^{-8}$	$8.99 \cdot 10^{-8}$
1.25 $\mu\text{m}$	$9.33 \cdot 10^{-7}$	$8.39 \cdot 10^{-7}$
0.75 $\mu\text{m}$	$3.41 \cdot 10^{-6}$	$2.87 \cdot 10^{-6}$
0.25 $\mu\text{m}$	$1.14 \cdot 10^{-5}$	$1.25 \cdot 10^{-5}$

Figure 4 indicates that the X-ray detection rates are increasing across all energy ranges, as seen in Table 1, as the tungsten target thickness decreases. Detected fluence of low energy photon from 1.5 to 3 keV increases dramatically. It is due to the higher the shielding efficiency of the tungsten target acting as a shielding material for the lower energy x-rays. Similarly, the maxima point of x-ray fluence shifts to the left as the thickness of tungsten decreases, which can also be explained by the same reason.

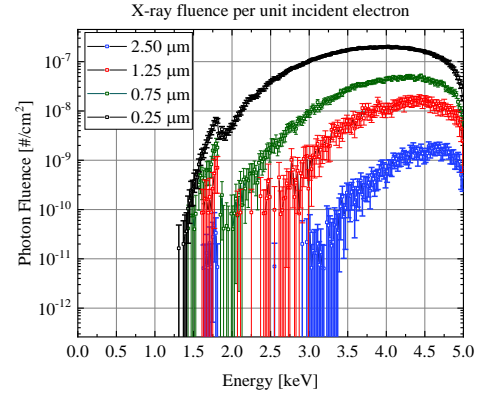


Fig. 4. Energy spectrum of X-ray Tube in respect to tungsten target thickness. The radiation shielding effect of a thick tungsten target reduces the amount of low-energy photons.

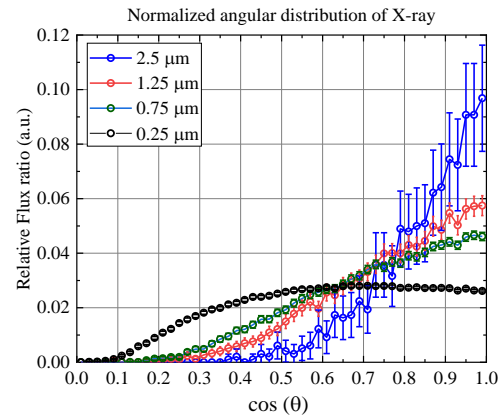


Fig. 5. Normalized angular distribution of x-ray in respect to tungsten target thickness. The shielding effect of a thick tungsten target attenuates photons deviating from the normal direction.

The effect of tungsten's x-ray shielding properties is also evident in the angular distribution. The following Figure 5 illustrates the angle distribution. The term  $\cos(\theta)$  corresponding to the abscissa of Figure 5 refers to the angle formed by the trajectory of the X-rays with respect to the normal of the tungsten target. Photons that penetrate tungsten obliquely, compared to those perpendicular to the normal, must travel a relatively longer distance within the tungsten. This effect increases the attenuation distance due to tungsten, so the thicker the tungsten, the higher the proportion of particles penetrating closer to the normal to tungsten. Also, the angular distribution becomes uniform as the thickness of the tungsten film approaches the traverse range of incident electrons.

#### **4. Conclusions**

After constructing the structure of the tube, we simulated the energy spectrum using Geant4. By comparing with MCNP6, we confirmed that proper physics models are adopted in the Geant4 toolkit. Through following simulation, we verified that the thickness of the tungsten target determines the amount of X-ray emission and scattering angle distribution. Therefore, the selection of an anode target width can characterize the x-ray tube's performance like sanitizing application. Experiments will be conducted to validate the simulation.

#### **ACKNOWLEDGEMENT**

This work was supported by the Research of Electron Beam and X-ray Emission Characteristics of CNT-Based Cold Cathode Tubes through aweXome Ray, Inc.

#### **REFERENCES**

- [1] Y. Sakai, A. Haga, S. Sugita, et al, Electron gun using carbon-nanofiber field emitter, Review of scientific instruments, 78.1. 2007.
- [2] J.W. Jeong, J.W. Kim, J.T. Kang, et al. A Vacuum-sealed compact x-ray tube based on focused carbon nanotube field-emission electrons. Nanotechnology 24.8, 2013.
- [3] S. Agostinelli, J. Allison, K. A. Amako, et al. GEANT4--a simulation toolkit, Nuclear Instruments and Methods In Physics Research section A:, 506,3, p. 250, 2003.
- [4] T. Goorley, M. James, T. Booth, et al. Initial MCNP6 release overview, Nuclear technology, Vol.180, p.298, 2012.
- [5] J. Baro, J. Sempau, J.M. Fernandez-Varea, et al. "PENELOPE: an algorithm for Monte Carlo simulation of the penetration and energy loss of electrons and positrons in matter", Nuclear Instruments and Methods In Physics Research section B:, 100.1, p. 31, 1995.
- [6] B.L. Henke, E.M. Gullikson, J.C. Davis, X-ray interactions: photoabsorption, scattering, transmission, and reflection at  $E = 50 - 30,000$  eV,  $Z = 1-92$ . Atomic data and nuclear data tables, 54.2, pp. 181, 1993.